An ESR Study on the Working States of a Pure V_2O_5 Crystal under the CO-oxidation

Yoshiya Kera* and Keiji Kuwata
Department of Chemistry, Faculty of Science, Osaka University, Toyonaka, Osaka 560

(Received August 29, 1978)

The V_2O_5 crystal, prepared from the pure V_2O_5 powder by a zone-melting method in the air, did not show any ESR signal. When the crystal came into contact with a mixture of CO and O_2 ($(CO/O_2) \geq 4$), an ESR spectrum with the hfs of 15-lines ($g_{//}=1.932$, $g_{\perp}=1.978$; $\langle g \rangle = 1.963$), which has been previously ascribed to an oxygen defect, was found at the beginning, but after prolonged contact a sharp spectrum ($\langle g \rangle = 1.954$) appeared. The intensity of the hf-lines was constant but that of the sharp spectrum increased with the contact time. The *g*-value and line shape of both spectra did not change with the contact time. The same spectra were also found in the crystal grown under a mixture of CO and O_2. On the thermal decomposition of pure NH_4VO_3 *in vacuo* a similar spectrum with a sharp line was found. The *g*-value became lower in the sample reduced further by SO_2 after the thermal decomposition. With reference to the data of TGA, DTA, magnetic susceptibility (χ_{mol}), and X-ray analysis of the vanadium oxides, the sharp spectrum was ascribed to a lower oxide or oxide state such as V_3O_7. Based on the ESR results, the working state of pure V_2O_5 crystal under CO-oxidation and its catalytic property are discussed.

Many phases, described by the general formulas of $V_{2m}O_{5m-2}$ (m=3, 4, (5), and 6)[1] and V_nO_{2n-1} (n= 3—9),[2,3] have been found for the vanadium oxides (V_2O_5–V_2O_3). The phase transitions between them have been well explained by the insertions and eliminations of the oxygen planes through the crystal from one side to the other, that is, by "shear planes."[4,5] The excellent properties of the vanadium oxides as catalysts,[6–8] for instance, high selectivities on the partial oxidations of hydrocarbons and the very long life, have been connected to this feature of the vanadium oxides, that the insertions and the eliminations of the oxygen can occur easily and reversibly during the phase transitions. Many authors[9–20] have discussed the catalytic mechanisms and the working states of vanadium oxide catalysts.

Recently, the X-ray analyses on the crystal structures of V_3O_7[21] and V_4O_9[22] have been accurately done. The crystal structures of the oxides were not so simple as to be induced from that of V_2O_5 based on the idea of the shear plane. The recent TGA and DTA studies on the vanadium–oxygen system have shown that the appearances and disappearances of the intermediate phases depend delicately upon the experimental conditions.[23–25] Furthermore, it has recently been made clear that vanadium oxides easily take several kinds of metals into the lattices and form several types of "vanadium bronzes."[26] The properties of the bronzes complicatedly depend upon the kinds and the contents of metallic impurities. Therefore, catalytic properties of vanadium oxide should be further investigated by taking the results, obtained recently on the oxide, into consideration.

Our kinetic work,[27] which was carried out on several types of the V_2O_5 crystals over wide ranges of the (CO/O_2) ratios, the total pressures, and the temperatures, suggested that even small amounts of metal impurities gave great effects to the catalytic activities and to the working states of the surface. Especially, it was noticed that, during the course of CO-oxidation on the highly purified thin plate crystallines of V_2O_5, the activation energy changed abruptly from a low (2.3 kcal/mol) to a high value (29 kcal/mol) even under the stoichiometric mixture of CO and O_2; the (CO/O_2)=2.1. The change in the activation energy suggested the change in the working state from V_2O_5 to some lower oxide.

In the present paper, the working states of the highly purified V_2O_5 crystal during the CO-oxidation was investigated by means of ESR spectroscopy. The problem of which phase or state of vanadium oxides is effective for promoting the catalysis is discussed, especially for the pure crystal.

Experimental

Materials. NH_4VO_3 was chemically purified according to the procedures of McCarley *et al.*[28] and Haemers.[29] Pure V_2O_5 powder was obtained by the thermal decomposition of the purified NH_4VO_3. The single crystals of the pure V_2O_5 were prepared by a zone-melting method, as is mentioned in detail below.

Procedures. The single crystals of V_2O_5 were prepared as follows: a Pt-boat, which contained the purified V_2O_5 powder of about 5.3 g, was placed in a quartz tube (volume, *ca.* 157 cm³) and then a zone-melting furnance was driven along the quartz tube. The atmosphere in the tube was controlled by varying the ratio and the total pressure of the mixture of CO and O_2. In the preparation under the air, one end of the tube was opened to the air. The width of the melting zone and the maximum temperature in the zone were 1.5 cm and 720 °C, respectively.

The single crystal of V_2O_5, which was prepared in the air and cut down in the proper size, was taken into a quartz tube (0.4 cm in inner diameter) for the measurement of ESR. The tube was gradually jointed with a glass tube (0.8 cm in the inner diameter) for the connection to a vacuum line. After the sample tube was heated preliminarily *in vacuo*, a given amount of the reaction gas was introduced at room temperature, and then the tube was sealed. The reaction tube was heated and was quenched in ice–water just before the ESR measurements. The reaction conditions are summarized in Table 1.

Some purified NH_4VO_3 powder, 0.123 g, was taken in each of the three quartz tubes for the ESR measurements. One of the tubes was opened to the air and the others were connected to a vacuum line. They were heated at 550 °C for 3 h. After heating, both the open tube and one of the

Table 1. The conditions of the contact of the pure V_2O_5 crystals with the reactants of CO and O_2
(Volume of ESR measurement tube sealed: 4 cm^3, temperatures: 460 and 560 °C)

Sample	CO Torr	O_2 Torr	(CO/O_2)	V_2O_5 g	("excess-CO"/V_2O_5)[a] mole ratio
S-S-1	330	20	16	0.182	0.07
S-S-2	352	88	4	0.182	0.04
S-S-3	88	22	4	0.115	0.016
S-S-4	32	8	4	0.115	0.006

a) "excess-CO": the amount of CO which remained after the equilibrium of the CO-oxidation, $CO+O_2/2=CO_2$, was achieved.

Table 2. ESR spectra in the pure V_2O_5 crystals grown under various atmospheres

Conditions of preparation	ESR parameters		Line widths (mT)[a]	
	g-tensor $\langle g\rangle$	A-tensor $\langle A\rangle$(mT)	low field	high field
In air	No spectrum			
$CO/O_2=4$, 200 Torr	1.964 $(g_{//}\approx 1.939$ $g_{\perp}\approx 1.976)$	5.8 $A_{//}\approx 8.2)$ $A_{\perp}\approx 4.6)$	—	—
$CO/O_2=16$ 350 Torr	1.954	—	3.1	4.3

a) The distances from the low field peak of the first derivative curve of the spectrum to the center and from the center to the high field peak were indepently estimated in the estimation of the line width.

evacuated tubes were sealed and then the ESR were measured. The other evacuated tube was filled with SO_2 gas at 724 Torr (1 Torr$=1.333\times 10^2$ Pa) after it was cooled down to room temperature and then was sealed. The inner volume of the tube was about 4 cm^3. The sample tube was again heated at 585 °C and, after quenching the tube in ice–water, ESR measurements were done.

ESR Measurements. ESR measurements and the determinations of the spin concentrations were done with the same procedure as was mentioned in the previous papers.[30)]

Results

ESR Spectra in the V_2O_5 Crystal Prepared under Various Atmospheres. No ESR spectrum was found for the V_2O_5 crystal prepared in the air. In the V_2O_5 crystal prepared under the mixture of CO and O_2 $(CO/O_2=4)$ at the total pressure of 200 Torr, however, a spectrum with the well-resolved hfs of 15-lines ($A_{//}=8.2$, $A_{\perp}=4.6$ mT) was found, as was illustrated in Fig. 1(a). On the other hand, in the crystal, prepared under the mixture of CO and O_2 $(CO/O_2=16)$ at the total pressure of 350 Torr, a new sharp line appeared near the center of the hfs of 15-lines, as was shown in Fig. 1(b). In this case, the resolution of the hfs-lines was also good, although the crystallinities seemed to be not so good as for the single crystal.

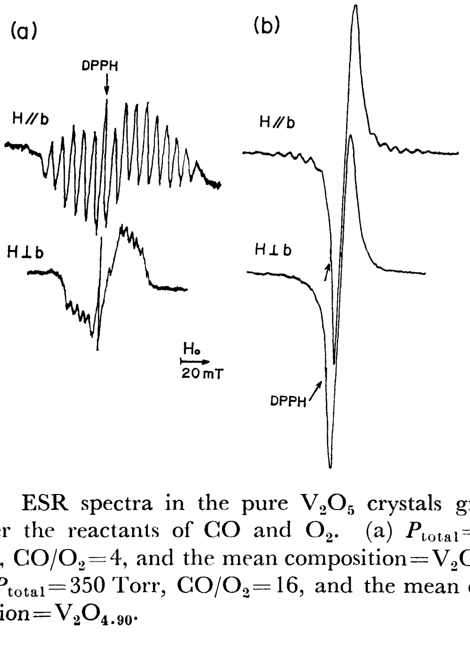

Fig. 1. ESR spectra in the pure V_2O_5 crystals grown under the reactants of CO and O_2. (a) $P_{total}=200$ Torr, $CO/O_2=4$, and the mean composition$=V_2O_{4.975}$ (b) $P_{total}=350$ Torr, $CO/O_2=16$, and the mean composition$=V_2O_{4.90}$.

Those samples showed neither fine structure nor the half resonance in ESR due to the spin-spin interaction for the spin state of $S=1$ or higher. Thus, both spectra could be ascribed to the state of $S=1/2$.

The ESR parameters—the g-values, hf-coupling constants, and the line widths—are given in Table 2. Table 2 indicates that the center of the sharp line differs a little bit from that of the hfs. The relative intensities of the hfs-lines to DPPH in Figs. 1(a) and 1(b) seem to be approximately equal to each other.

The ESR Spectrum for the Highly Purified V_2O_5 Crystal in Contact with the Mixture of CO and O_2. The ESR spectra which appeared for the pure V_2O_5 crystals in contact with the mixture of CO and O_2 are illustrated in Fig. 2. In the Figure, the larger the (CO/O_2) ratio and the total pressure and the longer the contact time, the larger the intensity of the sharp line becomes. In the S-S-4 after the contact of 49 h at 460 °C, only the spectrum with the hfs of 15-lines is seen, but in the S-S-3 after the contact of 49 h, a sharp line appeared together with the hfs-lines, although it is rather weak. In the S-S-2 after the contact of 72 h and in

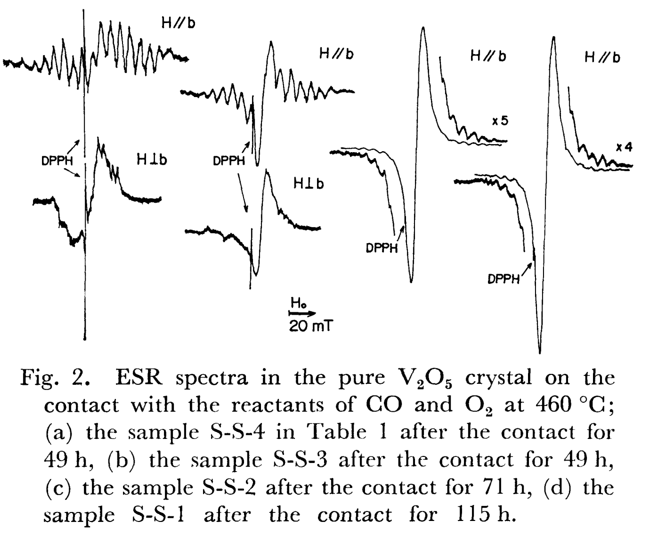

Fig. 2. ESR spectra in the pure V_2O_5 crystal on the contact with the reactants of CO and O_2 at 460 °C; (a) the sample S-S-4 in Table 1 after the contact for 49 h, (b) the sample S-S-3 after the contact for 49 h, (c) the sample S-S-2 after the contact for 71 h, (d) the sample S-S-1 after the contact for 115 h.

TABLE 3. ESR SPECTRA IN THE PURE V_2O_5 CRYSTALS IN CONTACT WITH THE REACTANTS OF CO AND O_2

Sample	Condition of reaction	ESR parameters		Line widths (mT)	
		g-tensor $\langle g\rangle$	A-tensor A(mT)	low field	high field
S-S-4	460 °C 49 h	1.963 $g_{//}\approx 1.932$ $g_{\perp}\approx 1.978$	 $A_{//}\approx 8.2$ $A_{\perp}$ —	—	—
S-S-3	460 °C 49 h	1.954	—	37	43
S-S-1 —S-S-4	460 °C 250 h	1.954 ±0.002	—	34	50
S-S-1 —S-S-4	560 °C 240 h	1.954 ±0.002	—	34	47

the S-S-1 after the contact of 115 h, the intensity of the sharp line increased considerably.

Figures 2(a)—2(d) indicate that the intensity of the sharp line increases depending upon contact time and the amount of the excess-CO, and, on the other hand, that of the hfs-lines does not depend on the contact time or on the amount of the excess-CO. This is seen in comparisons of the intensities of the spectra with that of DPPH. During the contact for 250 h an increase in the intensities of the sharp spectrum was found in all samples, S-S-1—S-S-4, but the line shape and the position of the center did not deviate from those at the very start. Even during further contact for 240 h at 560 °C, the intensities of the spectrum in all samples still increased and the shape and the position of the center were also kept constant. The ESR parameters of the spectra are summarized in Table 3.

The line shape of the sharp spectrum varied with the temperature of the measurements : the linewidth became larger at 300 K than that at 77 K. As an example, the spectrum in the S-S-3 after the contact for 240 h at 560 °C is given in Fig. 3. The broadening of the spectrum at room temperature would be caused by the shortening of the spin-lattice relaxation time. The growth of the sharp spectrum in the S-S-1—the S-S-4 at 460 °C and 560 °C are shown in Fig. 4. The growth of the sharp spectrum is seen at 560 °C to be linear against the amount of the excess-CO for the contact for 240 h, but at 460 °C in the runs with the higher contents of CO (S-S-3 and S-S-4) such linearity is not found. These findings might correspond to the fact that at 460 °C the process in the reduction of the surface is more rapid than the process in the diffusion into the bulk, while at 560 °C both processes are comparable. Table 3 shows that the ESR parameters of the sharp spectrum are constant without regard to the intensity of the spectrum, as was pointed out above.

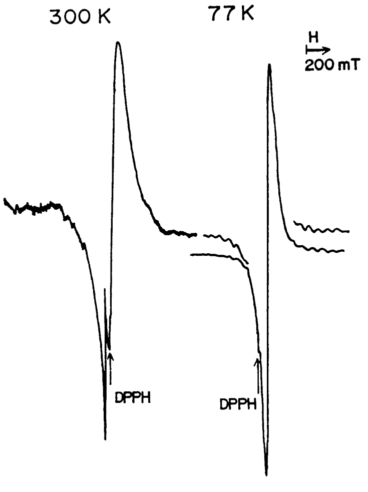

Fig. 3. The changes in the line width of the sharp spectrum with the temperatures of measurement.

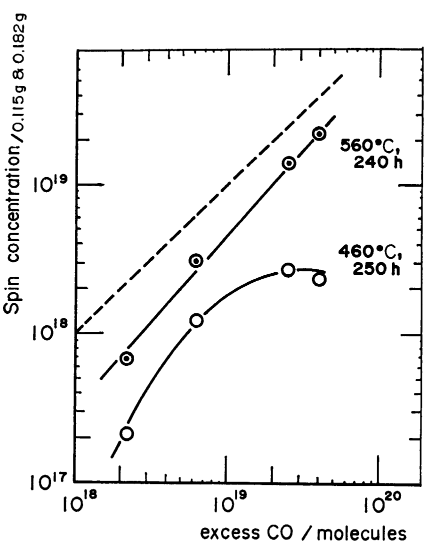

Fig. 4. The relations of the intensities of the sharp spectrum with the excess-CO. The dotted line indicates the spin concentration, expected in the crystal on complete consumption of the excess-CO.

After the contact with the mixture of CO and O_2 for a long time, the color of the crystal changed from bright brown to dark brown, but the brilliance of the (010) plane exposed to the surface from the start still remained after such treatments. The result was similar to that for the contact with the mixture of SO_2 and O_2.[30)]

ESR Spectra in the Vanadium Oxides, Obtained by the Thermal Decomposition of the Highly Purified NH_4VO_3 and Then by the Reduction with SO_2. In the sample obtained by the thermal decomposition of the purified NH_4VO_3 powder in the air, no ESR signal was found, *cf.* Fig. 5(a). After treatment of the sample with SO_2

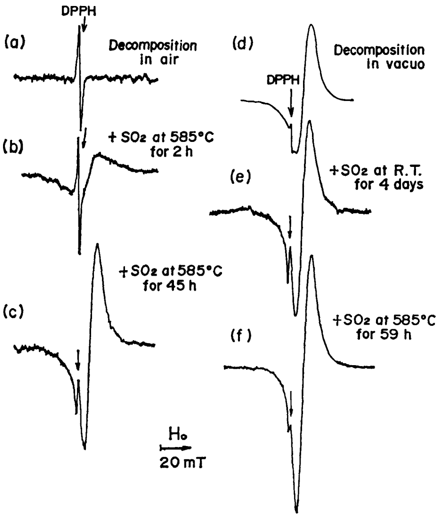

Fig. 5. ESR spectrum found on the thermal decompositions of the pure NH_4VO_3 and then the changes in the spectrum by the contact with SO_2.

at 585 °C, an ESR spectrum grew, as illustrated in Figs. 5(b) and 5(c). In the sample obtained by the thermal decomposition under a vacuum, an ESR spectrum appeared, as is shown in Fig. 5(d). By further treatment of the sample by SO_2, the spectrum changed, as illustrated in Figs. 5(e) and 5(f).

Discussion

The ESR Spectra in the CO–O_2–V_2O_5 System. The ESR spectrum with the hfs of 15-lines was found in the V_2O_5 crystal, which was prepared under the mixture of CO and O_2 (rather weakly reductive), as is shown in Fig. 1(a). After the contact with the mixture of CO and O_2 for a short time, the same spectrum appeared in the crystal in which no ESR signal had been detected initially as is shown in Fig. 2(a). A quite similar spectrum has also been found in the crystal treated with a mixture of SO_2 and O_2 at the initial stage. The spectrum was assigned to a V^{4+}—V^{5+} pair, accompanied by an oxygen defect.[30] On the other hand, in the two cases in which the V_2O_5 crystal was prepared under the mixture of CO and O_2 (rather strongly reductive) and was brought into contact with such a mixture, a new sharp spectrum appeared in the crystal, together with the hf-lines, as shown in Figs. 1(b), 2(c), and 2(d). Since the centers of both spectra were different, the sharp line did not seem to be ascribed simply to the exchange narrowed line of the hfs of 15-lines. The sharp line could be ascribed to a lower oxide phase or a lower oxide state of vanadium oxides, by taking into consideration the results that the ESR parameters of the sharp spectrum are constant without regard to the intensity of the spectrum, as was mentioned above.

According to the phase diagram of the vanadium–oxygen system by Kachi and Kosuge *et al.*,[31] the only phase which can coexist thermodynamically with V_2O_5 is V_3O_7. They[8] also measured the magnetic susceptibility (χ_{mol}) of V_3O_7, V_6O_{13}, and VO_2 and estimated μ_{eff} by using these equations: $\chi_{mol}=C/T-\theta$ and $\mu_{eff}=2.83\sqrt{C}$. The μ_{eff} ($=1.32$) in V_3O_7 seems to be rather well in accordance with the μ_{calcd} ($=1.00$), calculated under the assumption that V^{4+} ions were isolated and their concentration was given by the composition of ($V_2O_4\cdot 2V_2O_5$). In the case of V_6O_{13} the μ_{eff} ($=1.92$) is not very consistent with the μ_{calcd} ($=1.41$) calculated using similar procedures, and in the case of VO_2 the μ_{eff} ($=2.96$) and the μ_{calcd} ($=1.73$) are quite different from each other. In V_6O_{13} and VO_2, therefore, the spin state of V^{4+} ions in the crystals would not be so simple as that of V_3O_7. From these considerations, the sharp spectrum can be ascribed to the V_3O_7 phase. The slight difference between the μ_{eff} and μ_{calcd} in V_3O_7 suggests that V^{4+} ions are not isolated completely in the V_3O_7 phase. If the V^{4+} ions were isolated completely in the crystal, it should give the hf-coupling with a nuclear spin of ^{51}V ($I=7/2$) and thus the hfs of 8-lines should be found. But infact only a sharp line has been found because of the exchange narrowing.

On heating the pure V_2O_5 crystal at 160 °C and 300 °C under high vacuum (10^{-6} Torr) for a long period, Gillis and Boesman[38] observed the growth of a new sharp spectrum, the center of which was approximately consistent with that of hfs of 15-lines. From the consistency of both centers of the spectra, the growth of the spectrum seems to correspond to a preliminary step before the phase transition, $V_2O_5 \rightarrow V_3O_7$: for instance, the clustering of the oxygen vacancies.

The ESR Spectra Found for the Thermal Decompositions of the Pure NH_4VO_3 and Then for the Reductions by SO_2. In the DTA and TGA studies on NH_4VO_3 by Taniguchi *et al.*,[24] NH_4VO_3 changed to V_2O_5 by the decompositions in the air stream and to V_3O_7 *in vacuo.* Furthermore, their results suggested that the V_3O_7 was reduced to V_6O_{13} by a butadiene stream, and the V_2O_5 was reduced by SO_2 stepwise : $V_2O_5 \rightarrow V_4O_9 \rightarrow V_6O_{13} \rightarrow VO_x$ ($x \fallingdotseq 2$). With reference to these results, the changes in the ESR parameters with the thermal decompositions and then with the reductions by SO_2, as shown in Table 4, might be explained as follows. The spectrum of $\langle g \rangle = 1.956$, obtained on the thermal decomposition *in vacuo,* is ascribed to the V_3O_7 phase and the decrease in the *g*-value on the reduction by SO_2, $\langle g \rangle = 1.956 \rightarrow 1.947$, is caused by the process, $V_3O_7 \rightarrow$

TABLE 4. THE ESR SPECTRUM FOUND FOR THE THERMAL DECOMPOSITION OF A PURE NH_4VO_3 AND THE CHANGE IN THE SPECTRUM WITH THE REDUCTION BY SO_2

Condition of reaction	ESR parameter *g*-tensor $\langle g \rangle$	Line widths (mT)	
In air dec	No spectrum		
$+SO_2$ heating for 45 h	1.949	4.9	5.4
Evac. dec	1.956	4.2	6.2
$+SO_2$ at RT standing for 4 days	1.953	4.6	5.3
$+SO_2$ heating for 59 h	1.947	4.5	6.0

V_4O_9 or V_6O_{13}. The decrease in the *g*-value, accompanied by the appearence of some lower oxides or some lower oxide states, can be understood by taking a change in the symmetry of the crystal field around the vanadium(IV) ion into consideration, as is discussed below.

The V_2O_5 crystal is constructed from a kind of octahedron unit, which distorts quite a bit, as shown in Fig. 6.[32)] In VO_2 (rutile type)[33)] the octahedron is close to a proper one. In the intermediate phases : V_3O_7,[21)] V_4O_9,[22)] and V_6O_{13},[34)] three or four types of the octahedron unit are contained in the crystals. To show the comparisons of the V–O distances in the octahedron among the phases, Table 6 was prepared. For the intermediate phases, the V–O distances were evaluated as the simple means of those in all octahedrons. In Table 6, the V–O(1) increases gradually, except for the V_6O_{13}, and on the contrary the V–O(6) decreases with the progress in the reduction. This means that the octahedron in the vanadium oxides changes gradually from a highly distorted structure to a proper one with the progress in the reduction, that is, the degree of the deviation of the V(IV) ion from the O(2)–O(3)–O(4)–O(5) plane becomes small, except for V_6O_{13}. The crystal field splittings of V(IV) ions in TiO_2(rutile) and VO_2 crystals have been given by Simizu[36)] and Grunin *et al.*,[37)] as in Fig. 7(a). In the higher oxides the splittings probably change as in Fig. 7(b), because the V(IV) ion deviates further up from the oxygen square plane. The higher the oxidation states, the larger the δ becomes, while the Δ becomes a little smaller (or remains almost constant). The *g*-value can be roughly estimated by the familiar equations : $g_{zz}=g_0-4\lambda/\Delta$, $g_{xx}=g_0-\lambda/\delta_1$ and $g_{yy}=g_0-\lambda/\delta_2$, where λ is the spin-orbit coupling constant. Therefore, with the progress in the reduction, the following changes in the *g*-values will be expected : g_{zz}→increase slightly (or remain constant), and g_{xx} and g_{yy}→decrease quite a bit.

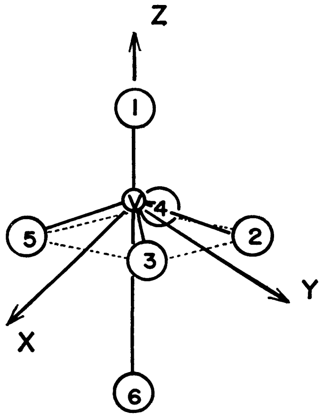

Fig. 6. The VO_6 octahedron unit in V_2O_5 crystal (Ref. 32); small circle: vanadium ion and large circle: oxygen ions.

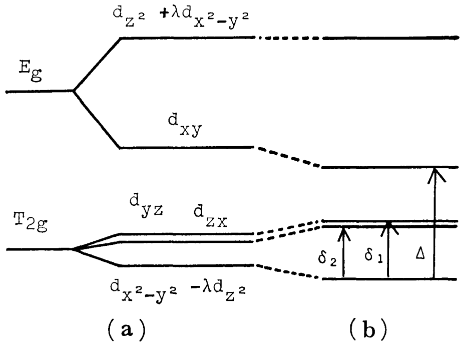

(a) (b)

Fig. 7. Schematical view on the changes in the energy diagram for the d-orbitals of the vanadium ion in the VO_6 octahedron with the progress in the oxidation and the reduction of vanadium oxides; (a) the energy diagram for the VO_6 unit in the VO_2 crystal (Refs. 36 and 37) and (b) that in higher oxides than VO_2.

For the V(IV) ion in the V_2O_5 crystals, $\langle g\rangle \fallingdotseq 1.975$ and g_{xx}, $g_{yy}>g_{zz}$ have been reported.[38)] On the other hand, in the V(IV) ion in VO_2 crystal, $\langle g\rangle=1.916$ was given.[37)] The *g*-values of the V(IV) ions deped in TiO_2, SnO_2, and GeO_2 were $\langle g\rangle=1.927$, 1.928, and 1.935, respectively.[39)] The tendency of the changes in the *g*-values is quite consistent with that expected above. The *g*-value in the spectrum found for the thermal decomposition of NH_4VO_3 *in vacuo*, $\langle g\rangle=1.956$, and also that for the reduction by SO_2, $\langle g\rangle=1.947$, given in Table 4, are also well understood according to the above discussion. That is, the changes in the *g*-values from 1.975 to 1.956 may correspond to the process, V_2O_5→V_3O_7, and the change from 1.956 to 1.947, to the process, V_3O_7→V_4O_9 or V_6O_{13}.

Recently, Kawashima *et al.*[25)] examined in detail the process of the reduction of V_2O_5 by SO_2 by means of the TGA and the X-ray analysis. The processes

Table 5. The comparisons of the V–O distances among the VO_6 octahedron units contained in the vanadium oxides between V_2O_5 and VO_2 (V_3O_7, V_4O_9, and V_6O_{13} are constructed from two or three kinds of the octahedron units. The simple mean values of the octahedrons were given in the oxides.)

Compound	$V\text{-}O_1$	$V\text{-}O_2$	$V\text{-}O_3$	$V\text{-}O_4$	$V\text{-}O_5$	$V\text{-}O_6$	Ref.
V_2O_5	1.595	1.780	1.878	1.878	2.021	2.785	32)
V_3O_7	1.624	1.812	1.946	1.952	1.984	2.690	21)
V_4O_9	1.629	1.891	1.897	1.931	1.974	2.531	22)
V_6O_{13}[a)]	1.906	1.835	1.865	1.835	2.086	2.375	34)
VO_2(rutile)	1.76	1.87	1.86	2.01	2.03	2.05	33)

a) Since certain values of the V-O distances have not been given for the V_6O_{13}, the authors estimated roughly, according to the data of Aebi.

in the reduction were found to occur stepwise and the phases described by the general formula of V_nO_{2n-1} appeared successively. However, the appearance and disappearance of the intermediate phases depended delicately and complicatedly upon the experimental conditions: for instance, the flow rates of the reductants, the partial pressures, the temperatures, the states of the pilling of the powder, and so on. According to their results, the present ESR spectra and the parameters found on the thermal decomposition of NH_4VO_3 and then on the reduction, are probably composite values.

The Growth of the V_2O_5 Crystal and Its Coexisting Phase under Oxidative and Reductive Atmospheres. Similar spectra to those shown in Figs. 1(a) and 1(b) have been found in the pure and doped V_2O_5 crystals. Ioffe *et al.*[38] have regarded the spectrum as caused by metal impurities, since the spectrum became more intensive in proportion to the contents of metal impurities. On the other hand, the spectrum was ascribed to the oxygen defect by Gillis *et al.*,[38] as was mentioned above. The fact that no ESR signal was found in the crystal of the V_2O_5 prepared in the tube opened to the air suggests that the concentrations of the impurities and the oxygen defects were below the sensitivity in the detection, that is, the starting material had been fully purified and the growth of the single crystal was accomplished under the condition of equilibrium. It means, furthermore, that the equilibrium pressure of the oxygen at the decomposition of the non-stoichiometric phase ($V_2O_{5-\delta}$) was very low, as compared to the partial pressure of oxygen in the air even at such a high temperature as the melting point of the V_2O_5 (*ca.* 670 °C).

In the case of the crystal prepared under the mixture of CO and O_2 ($CO/O_2=4$) at the total pressure of 200 Torr, only the spectrum ascribed to the oxygen defect was found, as discussed above. Since in the system the (excess-CO/V_2O_5) ratio is estimated to be 0.025, the non-stoichiometric region of V_2O_5 will extend at least up to $V_2O_{4.975}$ near the temperature of 670 °C. On the other hand, in the crystal prepared under the mixture of CO and O_2($CO/O_2=16$) at the total pressure of 390 Torr, a strong sharp spectrum, ascribed to a phase like V_3O_7, appeared in addition to the hfs-lines, as discussed above. In this case, the (excess-CO/V_2O_5) ratio was estimated to be 0.10. Thus the composition of $V_2O_{4.90}$ should be realized, if the equilibrium between the gaseous phase and the solid has been kept fixed throughout the crystal growth. That is, the non-stoichiometric phase of V_2O_5 would not extend up to $V_2O_{4.90}$.

The Change in the Surface States of the Highly Purified V_2O_5 Crystal during the CO-oxidation. The pure V_2O_5 crystal, kept under the conditions of the CO-oxidation (rather reductive atmosphere), showed a sharp spectrum, accompanied with the spectrum with the hfs of 15-lines. The line shape and the *g*-value of the ESR spectra were completely consistent with that in the crystal grown under a similar atmosphere. Both the line shape and the $\langle g \rangle$ were kept constant from the beginning of the appearence without depending on the (CO/O_2) ratio, the partial pressures of CO, the temperatures, or the reaction time. From the beginning the center of the sharp spectrum already differed from that of the hfs-lines, as seen in Fig. 2(b) and Table 3. This finding suggests the coexistence of the non-stoichiometric phase of the V_2O_5 and the V_3O_7 near the surface from the initial stage of the reduction. The intensity of the sharp lines increased gradually with the time, while that of the hfs-lines did not vary, as the comparison of the intensity with DPPH in Figs. 2 and 3 will show. This means probably that the other phases of the lower oxides did not exist in the crystal even locally. This idea will be supported by the fact that, although the color of the crystal varied from bright brown to dark brown, the brilliance of the (010) surface was always kept. The results of the isotopic exchange of oxygen also suggest that the mobility of the lattice oxygen was stimulated abruptly at above 500 °C.[40] Therefore, at least at such a high temperature as 560 °C, the highly purified V_2O_5 crystal is reduced homogeneously and gradually from the surface toward the bulk during the CO-oxidation (under rather reductive atmosphere).

The result obtained in a previous paper,[27] the abrupt change in the activation energy from the lower value to the higher during the CO-oxidation, could be related to the change in the surface states from the nonstoichiometric V_2O_5 to a lower oxides like as V_3O_7. The fact that, on the contrary, such a change in the working state was not seen for the unpurified crystal,[27] suggests that very little amounts of metal impurities play some important roles in preventing the change in working state. This subject is a future problem for the solid state chemistry on vanadium bronzes.

References

1) A. D. Wadsley, *Acta Crystallogr.*, **10**, 261 (1957).

2) S. Andersson and A. Magnéli, *Acta Chem. Scand.*, **8**, 1641 (1957); S. Andersson and L. Jahnberg, *Ark. Kemi.*, **21**, 413 (1966).

3) G. Andersson, *Acta Chem. Scand.*, **8**, 1599 (1954).

4) A. D. Wadslay, "Nonstoichiometric Compounds," ed by L. Mandelcorn, Acad. Press (1964).

5) J. S. Anderson and B. G. Hyde, *J. Phys. Chem. Solids*, **28**, 1393 (1967).

6) G. L. Simard, J. F. Steger, R. J. Arnott, and L. A. Siegel, *Ind. Eng. Chem.*, **47**, 1424 (1955).

7) E. Gillis, *Compt. Rend.*, **258**, 4765 (1964).

8) T. Toda, K. Kosuge, and S. Kachi, *Nippon Kagaku Zasshi*, **87**, 1311 (1966); S. Kachi, K. Kosuge, U. Shiotani, and N. Nakanishi, *Shokubai*, **10**, 1103 (1968); K. Kosuge, *J. Jpn. Soc. Powder and Powder Metal.*, **15**, 400 (1969).

9) P. Mars and D. W. Krevelen, *Chem. Eng. Sci. (Spec. Suppl.)*, **3**, 41 (1954).

10) V. A. Roiter, *Kinet. Katal.*, **1**, 63 (1960).

11) L. Ya Margolis, *Adv. Catal.* **14**, 429 (1963).

12) V. Ya. Vol'fson, L. N. Ganyuk, and E. F. Totskaya, *Kinet. Katal.*, **5**, 1100 (1964); V. Ya. Vol'fson, Ya. V. Zhigailo, E. F. Tatskaya, and V. V. Raksha, *ibid.*, **6**, 162 (1965).

13) T. Vrbaski, *J. Phys. Chem.*, **69**, 3092 (1965).

14) T. Seiyama, A. Suenaga, and W. Sakai, *Nippon Kagaku Zasshi*, **82**, 292 (1966).

15) H. Schaefer, *Ber. Bunzenges. Phys. Chem.*, **71**, 222 (1967).

16) G. K. Boreskov, *Kinet. Katal.*, **8**, 1020 (1967); **13**, 543 (1972).

17) G. L. Ross and P. H. Calderbank, *Chem. Eng. Sci.*, **26**, 2003 (1971).

18) W. M. H. Sachtler, *Catal. Rev.*, **4**, 27 (1971).

19) P. H. Emmett, *Catal. Rev.*, **7**, 1 (1973).

20) E. I. Andreikov, Yu. A. Sveshnikov, and N. D. Rusýanova, *Kinet. Katal.*, **15**, 1207 (1974); **16**, 919 (1975).

21) S. Andersson, J. Galy, and K. Wilhelmi, *Acta Chem. Scand.*, **24**, 1473 (1970); K. Waltersson, B. Forlund, K. Wilhelmi, S. Andersson, and J. Galy, *Acta Crystallogr.*, **30**, 2644 (1974).

22) K. Wilhelmi and K. Waltersson, *Acta Chem. Scand.*, **24**, 3409 (1970).

23) T. Sata, E. Komada, and Y. Ito, *Kogyo Kagaku Zasshi.*, **71**, 643 (1968); T. Sata and Y. Ito, *ibid.*, **71**, 647 (1968).

24) M. Kato, M. Taniguchi, and T. Kubo, *Kogyo Kagaku Zasshi*, **69**, 2102 (1966); M. Taniguchi, A. Miyazaki, and H. Yokomizo, *Shokubai*, **10**, 53 (1968); M. Taniguchi, S. Kato, and T. Nanao, *ibid.*, **14**, 53 (1972); H. Endo, M. Wakihara, and M. Taniguchi, *Chem. Lett.*, **1974**, 905.

25) K. Kawashima, K. Kosuge, and S. Kachi, *Chem. Lett.*, **1975**, 1131.

26) a) P. Hagenmuller, *Chem. Extended Defects in Non-Metallic Solids*, pp. 91—108, Amsterdam (1970); *Prog. Solid State Chem.*, **5**, 71 (1971); b) M. Nygren, *Chem. Commun. Univ. Stockholm*, 1 (1973).

27) Y. Kera, *Bull. Chem. Soc. Jpn.*, **52**, 888 (1979).

28) R. E. McCarley and J. W. Roddy, *J. Less-Common Met.*, **2**, 29 (1960).

29) J. Haemers, *Bull. Soc. Chim. Belg.*, **79**, 473 (1970).

30) Y. Kera and K. Kuwata, *Bull. Chem. Soc. Jpn.*, **50**, 2438, 2831 (1977).

31) K. Kosuge, T. Takada, and S. Kachi, *J. Phys. Soc. Jpn.*, **18**, 318 (1963); K. Kosuge, *J. Phys. Chem. Solids*, **28**, 1613 (1967).

32) a) A. Byström, K. Wilhelmi, and O. Brotzen, *Acta Chem. Scand.*, **4**, 1119 (1950); b) H. G. Bachman, F. R. Ahmed, and W. H. Barnes, *Z. Kristallogr.*, **115**, 110 (1961).

33) G. Andersson, *Acta Chem. Scand.*, **10**, 623 (1956).

34) F. Aebi, *Helv. Chim. Acta*, **31**, 8 (1948).

35) S. Westman, *Acta Chem. Scand.*, **15**, 217 (1961).

36) T. Shimizu, *J. Phys. Soc. Jpn.*, **23**, 848 (1967).

37) V. S. Grunin, V. A. Ioffe, and I. B. Patrina, *Phys. Status Solidi B*, **63**, 629 (1974).

38) a) J. L. Ragle, *J. Chem. Phys.*, **38**, 2020 (1963); b) E. Gillis and E. Boesman, *Phys. Status Solidi*, **14**, 337 (1966); c) V. A. Ioffe and I. B. Patrina, *Soviet Phys. Solid State*, **10**, 639 (1968); d) K. Hirota, K. Kuwata, and Y. Kera, *Bull. Chem. Soc. Jpn.*, **43**, 3017 (1970).

39) a) G. M. Zverev and A. M. Prokhorov, *Soviet Phys. -JETP*, **12**, 160 (1960); b) H. T. Gerritsen and H. R. Lewis, *Phys. Rev.*, **119**, 1010 (1960); c) C. Kikuchi, I. Chen, W. H. From, and P. B. Dorin, *J. Chem. Phys.*, **42**, 181 (1965); d) I. Siegel, *Phys. Rev. A.*, **134**, 193 (1964).

40) a) E. R. S. Winter, *Adv. Catal.*, **10**, 196 (1958); *J. Chem. Soc.*, 2889 (1968); b) G. K. Boreskov, *Adv. Catal.*, **15**, 285 (1964).